The effect of ultrasonic treatment on the mechanisms of grain formation of as-cast high purity zinc

B. Nagasivamuni, Gui Wang, David H. StJohn, Matthew S. Dargusch

PII: S0022-0248(18)30218-5
DOI: https://doi.org/10.1016/j.jcrysgro.2018.05.006
Reference: CRYS 24594

To appear in: *Journal of Crystal Growth*

Received Date: 16 February 2018
Revised Date: 30 April 2018
Accepted Date: 8 May 2018

Please cite this article as: B. Nagasivamuni, G. Wang, D.H. StJohn, M.S. Dargusch, The effect of ultrasonic treatment on the mechanisms of grain formation of as-cast high purity zinc, *Journal of Crystal Growth* (2018), doi: https://doi.org/10.1016/j.jcrysgro.2018.05.006

The effect of ultrasonic treatment on the mechanisms of grain formation of as-cast high purity zinc

Nagasivamuni B., Gui Wang, David H. StJohn, Matthew S. Dargusch

Centre for Advanced Materials Processing and Manufacturing (AMPAM), The University of Queensland, St Lucia QLD, 4072, Australia

Abstract

The potential for producing a large refined equiaxed zone by ultrasonic treatment (UST) of high purity zinc was investigated in order to improve the mechanical and formability performance. The macrostructure of cast ingots changed from large columnar grains without UST to three zones of fine columnar grains adjacent to the mould walls of the ingot, a refined equiaxed zone and a zone of a mixture of coarse equiaxed and columnar grains. A small zone of equiaxed grains was obtained when UST was applied during cooling from 440˚C to 419˚C for 2 minutes. The size of the equiaxed zone increased from about 20% of the casting's cross section to 50% when UST was applied for 3 or 4 minutes. In contrast, the application of UST for a longer time from a higher temperature (450˚C to 419˚C for 4 min) resulted in a smaller equiaxed zone of 18% indicating that a specific combination of UST time and temperature is required for the formation of a large equiaxed zone. The factors affecting the formation of the equiaxed zone throughout the solidification cycle are described.

Keywords: A1. Grain refinement, A2. ultrasonic treatment, B1. pure zinc, A1. solidification, A1. equiaxed and dendritic grains

1. Introduction

Zinc (Zn) and its alloys are primarily used to galvanize steel, a processing step that protects the steel against corrosion. Zinc alloys are also cast into gravity and pressure die cast parts,

used in the transportation and electronic industries as inexpensive mechanical parts. The main advantages of zinc-based alloys are low melting temperatures, good corrosion resistance, excellent machinability and wear resistant properties [1]. Wrought alloys are comprised of pure zinc and minor alloying elements such as Cu, Ti, Al and Pb because the unalloyed high purity Zn has a Hexagonal Close Packed (HCP) crystal structure and solidifies with a coarse grain structure both of which impairs sheet forming and deep drawing ability [2, 3]. Recently, considerable research on biodegradable metal implants identified Zn alloys as potential new-generation biomaterials. Zinc is biocompatible and critical to cellular growth, mitosis, fertility, immune system function, taste and smell, healthy skin and vision [4, 5]. However, the disadvantage of Zn as a biomaterial is that the mechanical properties are currently lower than that required for cardiovascular stents: yield strength of 200 MPa, tensile strength of 300 MPa and 18 to 20 % elongation [6, 7]. In order to improve the formability and mechanical properties of zinc alloys, achieving a fine, equiaxed grain structure in the as-cast condition is vital. Thus, it is important to understand the mechanisms that control the grain structure of Zn and its alloys during solidification [3, 8].

To obtain a fine equiaxed grain structure, it is well-established practice to add a grain refining master alloy that contains appropriate inoculants to promote heterogeneous nucleation, thus improving many properties of the as-cast metal and facilitating subsequent processing [3]. For instance, the addition of TiB_2 to certain Al alloys [9], Zr to Al-free Mg alloys [10] and Al – Ti or Zn – Ti master alloys to hypereutectic Zn – Al alloys [11, 12] results in the refinement of as-cast grain size. In the case of pure metals, planar solidification starts at the mold wall and when the melt is thermally undercooled, new spherical crystals may nucleate on potent nucleants in the liquid and grow as equiaxed grains [13]. However, in the case of pure Zn the HCP crystals grow in a dendritic form due to differences in the growth rate of some crystallographic directions compared with others [14]. The hexagonal unit cell along the c-

axis in Zn is distorted compared to HCP metals (c/a = 1.856 instead of 1.633) and because of this Zn is characterized by a large anisotropy of solid-liquid interfacial energy which in turn affects the growth of dendrites. Primary Zn dendrites at slow cooling rates preferentially grow in the $\langle 10\bar{1}0 \rangle$ direction with secondary arms in the $\langle 0001 \rangle$ direction [14, 15].

Liu et al. [16] reported that alloying elements such as Al and Mg refine the grain structure of cast Zn based on the growth restriction effect (Q) of solute additions. Some peritectic alloying elements (Cu and Ag) also introduce additional nucleation sites for better grain size reduction [16]. The disadvantages of adding or creating potent nucleant particles include: (1) dependence on alloy chemistry [3, 16]; (2) low efficiency, where it is often the case that only 1% of added particles are able to be active nuclei for the formation of grains [17]; (3) higher cost [10]; and (4) potential negative impacts on the corrosion resistance.

The requirement to find chemistry independent technologies has led to the development of refinement methods based on external fields including electromagnetic [18], pulsed magnetic fields [19-22], electric fields [23] and UltraSonic Treatment (UST) [24, 25]. Studies of dynamic conditions created by the external fields have reported that the formation of equiaxed grains may result from both increased nucleation rates and dendritic fragmentation. Fragmentation effects are generally explained as the breakage of dendrites from the mould walls or from large dendritic crystals within the cavitation zone and are then carried to the central region of the casting creating an equiaxed zone [19, 23, 26]. Some important mechanisms regarding enhanced nucleation related to electromagnetic and electric processing are explained as (i) enhanced undercooling by the Joule heating effect [20], (ii) decrease in the free energy for nucleation (ΔG) at lower undercooling [21] and (iii) decrease in the temperature gradient due to convection and associated induced thermal undercooling in pure metals that leads to more nucleation by reducing/delaying recalescence or remelting [22].

However, the third point also applies to UST [27-29]. UST is a powerful physical method for achieving fine grains in most alloys without the use of inoculants; it is a versatile technology that has gained significant interest due to its effectiveness in grain refinement and composite manufacturing reported in a wide range of Al- and Mg-based alloys [10, 24, 25]. Introducing ultrasound in the liquid melt causes acoustic cavitation (creation and implosion of bubbles) accompanied by a sudden local change in temperature and pressure conditions by several hundred orders of magnitude [30]. The localized high energy released due to cavitation is powerful enough to induce or assist nucleation processes and produce significant refinement in both primary crystals and intermetallic phases during solidification [31, 32]. Multiple violent acoustic cavitation events create pressure pulses that provide the undercooling required for enhanced nucleation described by the Clapeyron criterion [10, 33]. The asymmetrical collapse of bubbles creates microjets that erode any solid surface improving wetting of inactive substrates and the shockwaves assist dendritic fragmentation which could simultaneously increase the number of nuclei and grains [34, 35]. In addition, bulk acoustic streaming enhances convection and provides mass transport of the nucleated crystals throughout the effective volume bringing structural uniformity to the castings [28, 29, 36]. Under an ultrasonic field, it is difficult to identify a specific mechanism responsible for grain refinement, however, the overall conditions are advantageous for nucleation, fragmentation, transport and the survival of grains [25, 27-29, 37, 38]

Very few studies have demonstrated the potential of UST to refine Zn grains [39], however a systematic study is needed to understand the grain formation mechanisms during UST. The present work employs UST to refine the cast grain size of high purity Zn, with a goal to extend the application of UST to Zn based cast and wrought alloys. The roles of temperature and time during UST application on the formation of an equiaxed zone during solidification is investigated in this study providing mechanistic insights regarding Zn solidification.

2. Materials and Methods

850 to 900 grams of high purity Zn (99.995 wt.%) was melted in a boron nitride coated clay graphite crucible having outer dimensions of Ø 60 (bottom) × Ø 90 (top) × 95 mm in height and a wall thickness of 10 mm. An electric resistance melting furnace was used to melt unalloyed Zn at 500°C. After melting, the liquid metal was held for 15 minutes to stabilize the temperature and was then taken out of the furnace, skimmed and allowed to solidify in air under room temperature. A data acquisition system was employed to record the cooling curves for all samples at the rate of two readings per second using a K – type thermocouple placed slightly offset from the center of the crucible. A 1500 W piezoelectric transducer attached to a Ti alloy sonotrode was operated at a fixed power (0.65 KW) and amplitude (13 µm) for all UST experiments. The sonotrode was initially at room temperature and turned on when it first touches the melt surface while being lowered into the melt. Table 1 lists the casting conditions with sample code T representing the temperature when UST is applied and 1M to 4M for the time period in minutes when UST is applied. The total UST duration was divided into two regions above and below the equilibrium melting temperature (T_M) of 420°C for pure Zn. The area percentage of equiaxed grains for each condition are also given in Table 1. Fig. 1 (a) illustrates the selected temperature and time range of samples T430-1M to T450-4M within the crystallization regime of pure Zn. The solidified samples were sliced vertically and mechanically ground with abrasive sheets from 60 up to 1200 grit, followed by etching in a 50% HCl solution for macrostructure grain size analysis. As illustrated in Fig. 1(b), samples of 10 mm × 15 mm were taken from the Top (T), Middle (M) and Bottom (B) regions of each casting, were polished and anodized in a 4.6% HBF_4 solution at 15V for 25 s. A Leica Polyvar optical microscope was used to acquire microstructural images under polarized mode. Grain size and area number density of grains were measured as per the ASTM E – 112 standard [40].

3. Results and Discussion

3.1. Macrostructure and thermal analysis

Fig.1 (c and d) shows the macrostructure and microstructure of as-cast pure Zn (sample No UST) exhibiting directional growth of large columnar grains with an average grain size of 3065 ± 841 μm. The application of UST during cooling above the liquidus temperature did not refine the as-cast grain size, whereas when applied during the liquid to solid transformation below T_M without the presence of natural or added potent nucleant particles, refined equiaxed grains were produced as was observed for Al – Cu alloys [28, 29]. Therefore, for this study the range of temperatures selected for the application of UST listed in Table I, all fall across the melting point of Zn to include the onset of solidification as shown in Fig. 1(a).

The macrostructures presented in Fig. 2 (a – e) have three distinct zones: fine columnar grains adjacent to the edge of the casting; an equiaxed zone of refined grains above the columnar zone; and, above the white dashed line, are a mixture of large columnar and equiaxed grains. In all cases, an equiaxed zone is formed (Fig.2) and from sample T430-1M to sample T440-4M the size of the zone increases at the expense of the upper zone of mixed large columnar/equiaxed grains. Table I includes the thickness of the columnar zone formed adjacent to the vertical walls of the casting, which increases from sample T440-2M to T440-3M and T440-4M or T450-4M. Regardless of the initiation temperature the final thickness is related to the time of UST after T_M. The thickness of the columnar layer is negligible or thinner at the bottom of the casting which is probably due to the vigorous jet of hotter melt coming directly from under the sonotrode melting or detaching new grains from the bottom surface of the casting. By plotting the thickness of the columnar zone against time after T_M, and assuming the casting conditions are similar, the average growth rate of the columnar grains is calculated to be about 26 ± 6 μm s^{-1}.

The duration of UST before and after T_M is listed in Table 1 and plotted in Fig. 3 (a). The corresponding area percentage of the equiaxed zone is shown in Fig. 3 (b). For sample T430-1M, UST continued for only a short duration of 45s after T_M resulting in a small equiaxed zone covering 19% of the cross section area. Compared to the as-cast structure, the overall grain size is significantly reduced in sample T430-1M, however, it is mostly large dendritic grains. Interestingly, a fine columnar zone is not visible under the equiaxed zone indicating that the coolest starting temperature and/or the shorter UST duration of 45 s are insufficient to form a stable columnar zone. For sample T440-2M the duration of UST was extended to 90 s from 440°C and the size of the equiaxed zone increased from 19 % to 36 %. A further increase in the duration of UST to 132 s (T440-3M) and 203 s (T440-4M) increases the size of the equiaxed zone to approximately 55% and 47% respectively. A small equiaxed zone (18%) was observed for sample T450-4M similar to sample T430-1M implying that the number of grains generated by UST is not sufficient to create an equiaxed zone similar to that observed in T440-3M. As this result was not expected two additional castings subjected to the same conditions were made. All three castings show approximately the same macrographs in terms of area fraction of columnar, equiaxed and mixed zones. This result provides confidence of the repeatability of the testing method. Comparing the conditions of sample T440-4M with sample T450-4M, where UST was applied for a similar time after T_M, the only variable was an increase in the UST start temperature by 10°C, which caused a significant decrease in the size of the equiaxed zone reducing it from 55% to 18%. Overall, an increase in the size of the equiaxed zone is observed when the UST range of sample T440-2M is extended to T440-3M or T440-4M (Fig.2 (d) and (e)), however, the larger temperature range of UST above T_M for sample T450-4M results in a similar sized equiaxed zone to that of sample T430-1M (Fig.2 (c)). When the mixed columnar/equiaxed zone becomes smaller the ratio of equiaxed to columnar grains within this zone increases. This change is probably

related to the increased number of equiaxed grains produced after longer UST times more of which remain suspended after the majority of grains have settled into the equiaxed zone.

Fig. 4 (a) shows the cooling curves of the UST samples exhibit a sharp drop when the sonotrode is immersed in the melt at the start of UST and the corresponding endothermic peak is indicated in the first derivative curve in Fig. 4 (b). In the case of sample T450-4M, after the sudden temperature drop, the cooling rate quickly returns to the normal cooling rate indicative of a heated sonotrode, whereas for the rest of the UST samples the nucleation process of primary Zn occurs soon after the endothermic peak. The return to normal cooling implies the sonotrode temperature has stabilized so that heat extraction through the sonotrode is matched by heat provided by the bulk melt. A sonotrode that is a few degrees higher in temperature will reduce the driving force for grain formation and therefore decrease the number of grains formed per unit time, thus reducing the size of the equiaxed zone. In addition, a lower temperature difference between the undercooling beneath the sonotrode and the warmer bulk melt may cause a greater number of new grains to remelt further reducing the size of the equiaxed zone. Thus, in the case of pure Zn, selection of the temperature at which UST is applied when using an unpreheated sonotrode is critical for ensuring the largest equiaxed zone is formed.

3.2. Grain Formation, morphology and its growth

The heterogeneity of the grain microstructure was analyzed by considering the Top, Middle and Bottom regions as shown in Fig. 1(b), and the corresponding microstructures presented in Fig 5. The Top region under all UST conditions solidifies as a mixture of large equiaxed and columnar dendrites while fine grains are observed in the Bottom microstructures as they are all within the equiaxed zone. There exists a clear transition from the equiaxed zone to a large columnar/equiaxed zone in sample T440-2M and much finer grains were observed along the

boundary of this transition in samples T440-3M and T440-4M. The grain size and the area number density of grains per mm^2 measured across the regions are shown in Fig. 6 (a and b). Fig. 6 (a) shows that the grain size in the equiaxed zone decreases with UST time while Fig. 6 (b) shows the number density of grains increases as expected. The number of grains gradually increase for samples in the Top region except for sample T450-4M. A sharp linear increase in the number of grains is observed for samples T440-2M, T440-3M and T440-4M in the Middle region due to the upward shift across the micrographs of the boundary of the equiaxed zone with the mixed zone. After a steep increase in the number density from sample T430-1M to sample T440-3M, there is only a slight change in the Bottom region from sample T440-3M to sample T440-4M. Measurement of the number of grains in the solidified ingot is directly related to the number of grains that are able to survive and these UST operating conditions were found to be the best for achieving an equiaxed grain structure for pure Zn. Assuming that the grains are produced directly by UST during solidification with respect to the time after T_M, the number of grains formed is estimated for the T440 samples and shown in Fig. 7. The number of grains formed has a clear dependency on UST time increasing from T_M until UST is terminated for the regions plotted in Fig. 7.

Fig. 8 (a_1 to a_3) shows the morphology of grains in sample T440-2M gradually changed from nearly spherical equiaxed to an elongated morphology in samples T440-3M and T440-4M. While UST is being applied during solidification, some grains that are generated initially can grow and move within the melt and then settle out of the melt when UST is terminated. However, the grains generated just before UST was terminated are smaller and may settle more slowly. Thus, these smaller grains were found at the boundary between the equiaxed zone and the mixed zone observed in the Middle region. This is likely to be the reason for the gradual change in the morphology of equiaxed grains. The boundary between the equiaxed zone and the mixed columnar/equiaxed zone of sample T440-4M in Fig. 8 (b_1) shows a band

of grains that were likely to be the last to settle from the melt when UST was terminated. The grain size distribution (dotted area in Fig. 8 (b_1)) in Fig. 8 (b_2) shows that a grain diameter as small as 40 μm can be found in the boundary region. Immediately above this layer, the grains appear larger and dendritic towards the Top region of the melt (marked as 1 to 3 in Fig. 8 (b_1)). Fig. 8 (c_1) shows the dendritic grains with multiple branches. Because of the large anisotropy of the solid-liquid interfacial energy, Zn crystal growth exhibits a plate-like cellular structure. Under a magnetic field, it has been found that the primary trunks preferentially grow in a horizontal direction <0001> in the basal plane and then branched vertically in the $<10\bar{1}0>$ direction to produce another primary trunk [41]. This branched trunk can further create high order branches in the basal planes to enter into a new cycle [14]. Fig. 8 (c_2) shows the fully developed branches of the Zn dendrites and their preferential planes and directions are denoted in Fig. 8 (c_3). In this manner, the elongated grains in the equiaxed zone just below the boundary layer of small spherical grains would be the initial stages of forming the larger dendritic grains described above.

According to the research by Wang et al. [29] on Al – 2Cu alloys, UST applied from 40°C and 60°C above the liquidus and terminated just below the liquidus temperature (range II) resulted in significant refinement and produced an equiaxed structure throughout the casting volume. However, in the present study, UST started from 30°C above the melting point of pure Zn (sample T450-4M) and the microstructure mostly remains fully dendritic. Therefore, the solidification parameters reported for UST in Al alloys cannot be directly applied to the crystallization of Zn. Compared to Al alloys, the thermophysical properties such as thermal conductivity ($k_{solidAl}$ = 222 W/mK and $k_{solidZn}$ = 101 W/mK) and the melting temperature is low for Zn alloys [42]. Even in Al alloys, continuous operation with a pre-heated sonotrode causes slight grain coarsening [24]. A key difference is the presence of solute Cu which promotes nucleation by the formation of constitutional supercooling. The amount of

constitutional supercooling generated during grain growth also protects the grains from remelting [38]. It is expected that the addition of segregating solute elements to Zn will produce constitutional supercooling thus enhancing the effect of UST producing much larger equiaxed zones. Solute would also promote a columnar to equiaxed transition reducing the thickness of the columnar zone.

3.3. Mechanism of grain formation during UST

The factors affecting refinement during UST are described in the schematic diagram shown in Fig. 9. Based on the above discussion heat is being extracted during UST by the sonotrode and by the walls of the casting mould. The latter heat extraction causes a zone of columnar grains to form and this zone thickens until the growth of these grains are stopped by the sinking UST-generated equiaxed grains after UST is terminated. When the cold sonotrode is immersed into the melt, there is a sudden temperature drop (indicated by the derivative of the cooling curve in Fig. 4 (b)) which is likely to cause a small solidified layer to form immediately on the surface of the tip of the sonotrode (Fig. 9 (a)). The formation of solid crystals around a water cooled sonotrode has been reported to continuously contribute to the nucleation rate [43]. However, in the present work the use of cold sonotrode above T_M may release such clusters of solidified grains by strong cavitation which are then carried by acoustic streaming towards the bottom of the crucible and these grains will melt until the bulk melt temperature drops below T_M. This may occur under all the conditions of UST because sonication is initiated well above T_M. A high rate of convection created by acoustic streaming is established in the liquid within the effective volume [38]. Simultaneously, due to the difference in the thermal conditions available at the sonotrode - melt interface, continuous grain formation occurs in the interface region described in Fig. 9 (b). As the UST is operating at a temperature below T_M beneath the sonotrode while the melt temperature is above T_M for an initial period of time and, therefore, the survival of such grains is most probably very

short. This is the reason why, when UST ceases just before T_M, it does not have any influence on the final grain size [29].

One important assumption made here is that the powerful cavitation forces immediately below the sonotrode create spherical or nearly spherical crystals, because there is not much deviation observed in the morphology of the last to solidify fine equiaxed grains (Fig. 8 (b)).

Before T_M is reached the well-established acoustically generated convection pathway within the streaming volume illustrated in Fig. 9 (c, d) establishes a more uniform temperature field by reducing the temperature gradient. As the melt cools below T_M the temperatures along the gradient become undercooled below T_M. This situation enables the grains to survive as they are transported throughout the melt [27]. It should be noted that the sonotrode acts as a heat sink extracting heat from the melt which in turn generates more grains, whereas the walls of the crucible have been heated by the acoustic convection reducing the rate of heat transfer. For simplification, the present work assumes that the grains created are fine enough to be transported by convection until UST is terminated or until the crystals have grown sufficiently large to drop out of the convective flow field. This scenario is illustrated in Fig. 9 (c) where (i) the convection field is established with a temperature range that is sufficient to promote grain formation and ensure the survival of the grains, (ii) a greater number of crystals are being generated at or near the melt sonotrode interface and (iii) acoustic streaming assists the transportation of grains.

Considering the above explanations in terms of the final grain size achieved, for sample T430-1M, UST is initiated at a lower temperature difference ($\Delta T_{UTi} = 10$℃) where the crystals created at or near the sonotrode tip are quickly carried into the melt to form the equiaxed zone. Because UST is stopped 45 seconds after the melting point is reached and due to the difference in the density of solid (ρ = 7.14 g cm^{-3}) and liquid Zn (6.62 g cm^{-3}) [44] the

initially created fine, spherical grains will sink under the influence of gravity and the rest of the volume becomes depleted of many of the new grains and solidifies as a mixture of coarse columnar and equiaxed grains. It is interesting to note that the number of grains in the mixed zone is higher than those in the no-UST as-cast structure, meaning that settling does not occur rapidly leaving UST-generated grains to grow in this zone. On termination of UST, a sudden increase in the cooling rate causes the crystal growth rate to increase while the grains float down towards the bottom of the crucible.

For the family of samples T440-2M, 3M and 4M, the temperature difference of UST initiation ($\Delta T_{UTi} = 20$℃) is larger than that of sample T430-1M and also follows the path as shown in the Fig. 9 (a to c). Because the time taken after T_M is doubled for sample T440-2M compared to sample T430-1M, (Fig. 3) there is a notable increase in the size of the equiaxed zone from 19% to 36%. When this is continued to 132 s in sample T440-3M, the size of the equiaxed zone increases linearly to a maximum of 55%. The increase in total UST duration from sample T440-2M to T440-3M was only 1 minute which brings a 19 % increase in the size of the equiaxed zone (from 36 to 55 %). However, a further increase of 1 minute from sample T440-3M to sample T440-4M appears to slightly reduce the size of the equiaxed area (47%). An expected further increase of 19 % more equiaxed grains is not observed and this clearly indicates that the operating efficiency of the sonotrode has decreased. Microstructures at the interface between the equiaxed and mixed zones in sample T440-4M are shown in Fig. 9. The loss of expected refinement in sample T440-4M can be better understood by considering the result of sample T450-4M.

For sample T450-4M 87 s before reaching the T_M was much longer than any of the other UST samples (and $\Delta T_{UTi} = 30$℃) and thus the sonotrode may have been preheated to a higher temperature before grain formation begins. The cooling curve presented in Fig. 4(a) suggests that this might be the case. The schematic diagram shows that the path of UST

operation is now shifted from Fig. 9 (a, b) to 9 (d). While the sonotrode still acts as a heat sink, the temperature difference between the bulk melt and that directly under the sonotrode would be less which is indicated as being warmer in Fig. 9 (d). This smaller difference and the associated lower driving force (low undercooling) for grain formation would reduce the number of grains produced compared to the scenario illustrated Fig. 9 (c). This may also be the reason why there is no further increase in the size of the equiaxed region when the sonotrode operates from sample T440-3M to T440-4M because the sonotrode may be gradually becoming warmer and similar to that for the T450 condition.

The development of grains on or near the cooler tip of the sonotrode by intense cavitation in the undercooled zone below the sonotrode schematically shown in Fig. 9 is referred to as an enhanced nucleation mechanism of grain formation. This effect is powerful enough to produce more equiaxed or spherical grains in a small volume because the mechanism of dendritic breakage is found to be unlikely in producing spherical grains as reported for an Al – 10Cu alloy based on a study of secondary dendrite arm spacing measurements [45]. Although the sonotrode is preheated, it can still extract heat from the melt, which results in highly equiaxed grains [29, 46]. Most UST experiments undertaken on the small scale [10, 29, 45-47] have restricted their discussions to cavitation-induced nucleation based on the Clapeyron criterion or on cavitation bubble formation and collapse and dendrite fragmentation. However, the research by Ferguson et. al [46] listed a number of experimental variables including low pouring temperature and sonotrode condition affecting grain formation during UST. This is supported by the present work based on UST initiation temperature and a cooler sonotrode affecting equiaxed grain formation (compare samples T440-4M and T450-4M). It should be noted that even for a small volume the generation of equiaxed grains has limitations (T450-4M) which can be overcome through control of process parameters such as the type of transducer (e.g. water cooled), the volume

ultrasonically treated, intensity of vibrations and material properties (density, thermal conductivity and solute content of the alloy). The interpretations made in the present work are based on finding the optimum combination of time and temperature for a small scale ingot casting to understand the mechanisms controlling grain formation, which needs further exploration for large scale applications where maintaining a source for the formation of equiaxed grains is more challenging.

4. Conclusions

Pure Zn was ultrasonically treated over a range of temperatures and times. It was revealed that:

- In contrast to the solidification of pure Zn where very large columnar grains grow from the mould walls towards the hot zone at the top of the ingot casting, the application of UST formed three zones: a zone of fine columnar grains, an equiaxed zone of refined grains and a zone containing a mixture of large equiaxed and colmnar grains.
- The size of the equiaxed zone was affected by the time of UST application and the degree of superheat when UST begins. At superheats of 10 and 20^{o}C increasing the time of UST after reaching T_M from 45 to 203 s, is the dominant factor affecting the size of the fine columnar and equiaxed zones. When the superheat is 30^{o}C, the equiaxed zone is small. It is proposed that the increase in superheat increases the temperature of the sonotrode tip reducing the amount of undercooling resulting in less grains being formed and possibly increased remelting of newly formed grains.
- A columnar zone is formed adjacent to the ingot walls and is able to grow at an average rate of 26 μm s^{-1} before its growth is stopped by the settling of equiaxed grains when UST is terminated.

- The zone above the equiaxed zone is of much larger grains. The average grain size decreases with longer UST times which is proposed to be due to a larger number of UST generated grains remaining in this zone after most have sunk towards the bottom of the ingot. The last grains to settle at the top of the equiaxed zone are small and spherical indicating they were the last grains to be formed by UST before UST was terminated.
- Based on observation of the macrostructures and the shape of the equiaxed zone, grains formed under the sonotrode are then transported into the bulk of the melt by acoustically-generated convection. The continued growth of the grains is impeded by the adjacent suspended grains and as the number density of grains increases the final average grain size decreases. When UST is terminated the melt re-establishes a normal cooling condition while the grains suspended in the melt settle on top of the columnar zone.

Acknowledgements

The authors acknowledge the financial support of the ARC Research Hub for Advanced Manufacturing of Medical Devices and the ARC Discovery grant DP140100702.

References

[1] A.S.M.I.H. Committee, ASM Handbook, Volume 02 - Properties and Selection: Nonferrous Alloys and Special-Purpose Materials, in, ASM International, 1990, pp. 1118-1128.

[2] S.W.K. Morgan, Zinc and its alloys and compounds, John Wiley and Sons, New York, 1985.

[3] Z.L. Liu, D. Qiu, F. Wang, J.A. Taylor, M.X. Zhang, Grain refinement of cast zinc through magnesium inoculation: Characterisation and mechanism, Mater Charact, 106 (2015) 1-10.

[4] H.F. Li, Y.F. Zheng, L. Qin, Progress of biodegradable metals, Prog Nat Sci-Mater, 24 (2014) 414-422.

[5] P.K. Bowen, J. Drelich, J. Goldman, Zinc Exhibits Ideal Physiological Corrosion Behavior for Bioabsorbable Stents, Adv Mater, 25 (2013) 2577-2582.

[6] P.K. Bowen, E.R. Shearier, S. Zhao, R.J. Guillory, F. Zhao, J. Goldman, J.W. Drelich, Biodegradable Metals for Cardiovascular Stents: from Clinical Concerns to Recent Zn-Alloys, Adv Healthc Mater, 5 (2016) 1121-1140.

[7] J. Kubasek, D. Vojtech, E. Jablonska, I. Pospisilova, J. Lipov, T. Ruml, Structure, mechanical characteristics and in vitro degradation, cytotoxicity, genotoxicity and mutagenicity of novel biodegradable Zn-Mg alloys, Mat Sci Eng C-Mater, 58 (2016) 24-35.

[8] Z.L. Liu, D. Qiu, F. Wang, J.A. Taylor, M.X. Zhang, Effect of Grain Refinement on Tensile Properties of Cast Zinc Alloys, Metall Mater Trans A, 47a (2016) 830-841.

[9] M. Easton, D. StJohn, Grain refinement of aluminum alloys: Part I. The nucleant and salute paradigms - A review of the literature, Metall Mater Trans A, 30 (1999) 1613-1623.

[10] A. Ramirez, M. Qian, B. Davis, T. Wilks, D.H. StJohn, Potency of high-intensity ultrasonic treatment for grain refinement of magnesium alloys, Scripta Mater, 59 (2008) 19-22.

[11] W.A. Pollard, K.M. Pickwick, J.T. Jubb, R.H. Packwood, The grain refinement of zinc-aluminum alloys by titanium, Canadian Metallurgical Quarterly, 13 (1974) 535-543.

[12] S.Q. Yan, H.X. Wang, The Effect of Small Amount of Titanium Addition on the Grain Refinement and Mechanical Properties of ZA48 Alloy, J Mater Eng Perform, 22 (2013) 1113-1119.

[13] D.M. Stefanescu, Cellular and dendritic growth, in: Science and Engineering of Casting Solidification, Second Edition, Springer US, Boston, MA, 2009, pp. 1-38.

[14] L. Li, C. Ban, X. Shi, H. Zhang, M. Cai, H. Liu, J. Cui, H. Nagaumi, Crystallographic growth pattern of zinc-rich plate-like cells under a high magnetic field, Mater Lett, 185 (2016) 447-451.

[15] A. Durussel, Influence of Zinc Anisotropy on Solidification Microstructures: Experimental Results and Phase-Field Simulations, in, EPFL, D.O.I 10.5075/epfl-thesis-6708, 2015.

[16] Z.L. Liu, F. Wang, D. Qiu, J.A. Taylor, M.X. Zhang, The Effect of Solute Elements on the Grain Refinement of Cast Zn, Metall Mater Trans A, 44a (2013) 4025-4030.

[17] D.H. StJohn, M. Qian, M.A. Easton, P. Cao, The Interdependence Theory: The relationship between grain formation and nucleant selection, Acta Mater, 59 (2011) 4907-4921.

[18] C. Vives, Electromagnetic refining of aluminum alloys by the CREM process: Part I. Working principle and metallurgical results, Metallurgical Transactions B, 20 (1989) 623-629.

[19] Y.-Y. Gong, J. Luo, J.-X. Jing, Z.-Q. Xia, Q.-J. Zhai, Structure refinement of pure aluminum by pulse magneto-oscillation, Materials Science and Engineering: A, 497 (2008) 147-152.

[20] Z. Zhao, Y. Liu, L. Liu, Grain Refinement Induced by a Pulsed Magnetic Field and Synchronous Solidification, Materials and Manufacturing Processes, 26 (2011) 1202-1206.

[21] Y.J. Li, W.Z. Tao, Y.S. Yang, Grain refinement of Al–Cu alloy in low voltage pulsed magnetic field, Journal of Materials Processing Technology, 212 (2012) 903-909.

[22] D. Liang, Z. Liang, Q. Zhai, G. Wang, D.H. StJohn, Nucleation and grain formation of pure Al under Pulsed Magneto-Oscillation treatment, Mater Lett, 130 (2014) 48-50.

[23] J. Li, J. Ma, Y. Gao, Q. Zhai, Research on solidification structure refinement of pure aluminum by electric current pulse with parallel electrodes, Materials Science and Engineering: A, 490 (2008) 452-456.

[24] D.G. Eskin, Ultrasonic processing of molten and solidifying aluminium alloys: overview and outlook, Materials Science and Technology, 33 (2017) 636-645.

[25] G.I. Eskin, Broad prospects for commercial application of the ultrasonic (cavitation) melt treatment of light alloys, Ultrason Sonochem, 8 (2001) 319-325.

[26] D.G. Eskin, I. Tzanakis, F. Wang, G.S.B. Lebon, K. Pericleous, P.D. Lee, T. Connolley, J. Mi, Fundamental Studies of Ultrasoinc Melt Processing, in: Z. Fan (Ed.) Proceedings of the 6th Decennial International Conference on Solidification Processing BCAST, Brunel University London, Old Windsor, UK, 2017, pp. 546 - 549.

[27] G. Wang, P. Croaker, M. Dargusch, D. McGuckin, D. StJohn, Simulation of convective flow and thermal conditions during ultrasonic treatment of an Al-2Cu alloy, Comp Mater Sci, 134 (2017) 116-125.

[28] G. Wang, Q. Wang, M.A. Easton, M.S. Dargusch, M. Qian, D.G. Eskin, D.H. StJohn, Role of ultrasonic treatment, inoculation and solute in the grain refinement of commercial purity aluminium, Sci Rep-Uk, 7 (2017) 9729.

[29] G. Wang, M.S. Dargusch, M. Qian, D.G. Eskin, D.H. StJohn, The role of ultrasonic treatment in refining the as-cast grain structure during the solidification of an Al-2Cu alloy, J Cryst Growth, 408 (2014) 119-124.

[30] J.H. Bang, K.S. Suslick, Applications of Ultrasound to the Synthesis of Nanostructured Materials, Adv Mater, 22 (2010) 1039-1059.

[31] L. Zhang, D.G. Eskin, L. Katgerman, Influence of ultrasonic melt treatment on the formation of primary intermetallics and related grain refinement in aluminum alloys, J Mater Sci, 46 (2011) 5252-5259.

[32] J.R.G. Sander, B.W. Zeiger, K.S. Suslick, Sonocrystallization and sonofragmentation, Ultrason Sonochem, 21 (2014) 1908-1915.

[33] M. Qian, A. Ramirez, A. Das, Ultrasonic refinement of magnesium by cavitation: Clarifying the role of wall crystals, J Cryst Growth, 311 (2009) 3708-3715.

[34] T.V. Atamanenko, D.G. Eskin, L. Zhang, L. Katgerman, Criteria of Grain Refinement Induced by Ultrasonic Melt Treatment of Aluminum Alloys Containing Zr and Ti, Metall Mater Trans A, 41a (2010) 2056-2066.

[35] G. Wang, M.S. Dargusch, D.G. Eskin, D.H. StJohn, Identifying the Stages during Ultrasonic Processing that Reduce the Grain Size of Aluminum with Added Al3Ti1B Master Alloy Advanced Engineering Materials, 19 (2017) 1700264-n/a.

[36] G. Ruecroft, D. Hipkiss, T. Ly, N. Maxted, P.W. Cains, Sonocrystallization: The Use of Ultrasound for Improved Industrial Crystallization, Org Process Res Dev, 9 (2005) 923-932.

[37] G.I. Eskin, Cavitation Mechanism of Ultrasonic Melt Degassing, Ultrason Sonochem, 2 (1995) S137-S141.

[38] D.H. StJohn, A. Prasad, M.A. Easton, M. Qian, The Contribution of Constitutional Supercooling to Nucleation and Grain Formation, Metallurgical and Materials Transactions a-Physical Metallurgy and Materials Science, 46a (2015) 4868-4885.

[39] H.J. Seemann, H. Staats, K.G. Pretor, Verfahren zur Schwingungsbehandlung von Metall- und Stahlschmelzen unter besonderer Berücksichtigung der Kornfeinung durch Erstarrungsbeschallung, Archiv für das Eisenhüttenwesen, 38 (1967) 257-265.

[40] ASTM E 112- 13 Standard Test Methods for Determining Average Grain Size, in, West Conshohocken, PA, 2013, pp. 1-28.

[41] E.C. Rollason, R.R. Roberts, Effect of Cooling Rate and Composition on the Embrittlement of Weld Metal, J Iron Steel I, 166 (1950) 105-&.

[42] A.E. Ares, C.E. Schvezov, Influence of solidification thermal parameters on the columnar-to-equiaxed transition of aluminum-zinc and zinc-aluminum alloys, Metall Mater Trans A, 38a (2007) 1485-1499.

[43] V. Abramov, O. Abramov, V. Bulgakov, F. Sommer, Solidification of aluminium alloys under ultrasonic irradiation using water-cooled resonator, Mater Lett, 37 (1998) 27-34.

[44] F.C. Porter, Properties in Zinc Handbook: Properties, Processing, and Use in Design, Marcel Dekker, New York, 1991.

[45] H.R. Kotadia, M. Qian, D.G. Eskin, A. Das, On the microstructural refinement in commercial purity Al and Al-10 wt% Cu alloy under ultrasonication during solidification, Mater Design, 132 (2017) 266-274.

[46] J. Ferguson, B. Schultz, K. Cho, P. Rohatgi, Correlation vs. Causation: The Effects of Ultrasonic Melt Treatment on Cast Metal Grain Size, Metals-Basel, 4 (2014) 477.

[47] X.B. Liu, Y. Osawa, S. Takamori, T. Mukai, Grain refinement of AZ91 alloy by introducing ultrasonic vibration during solidification, Mater Lett, 62 (2008) 2872-2875.

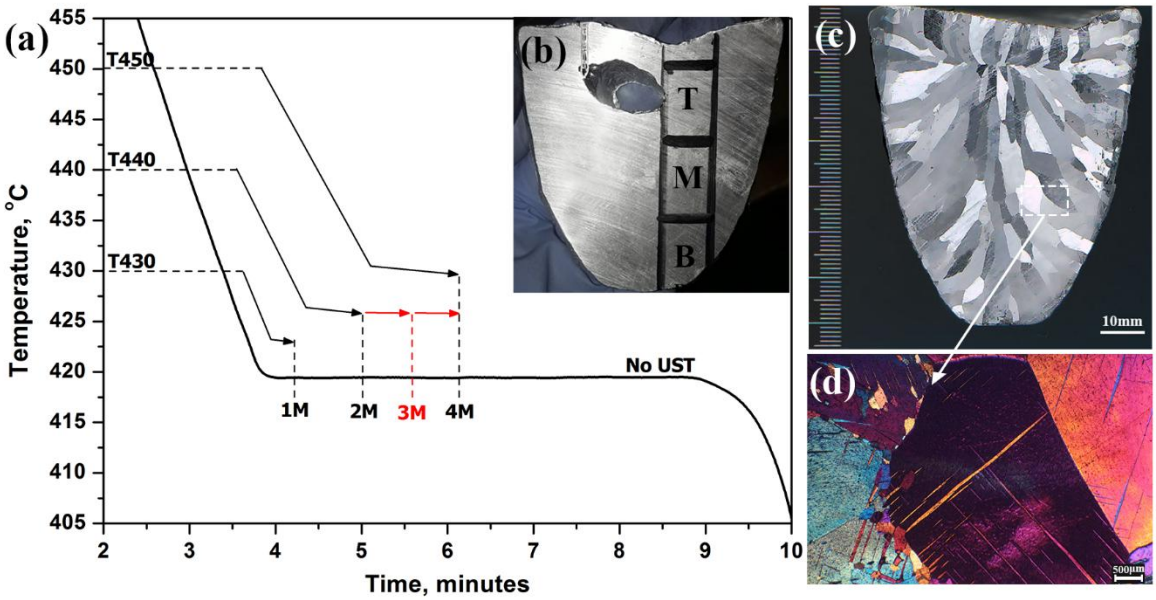

Fig.1 (a) The cooling curve of pure Zn illustrating the experimental conditions where T430 to T450 is the temperature at which UST is started and 1 to 4M is the duration over which UST is applied, (b) the regions T, M and B corresponds to the top, middle and bottom regions subjected to microstructure analysis (c and d) shows the macrostructure and microstructure of as-cast pure Zn (no UST)

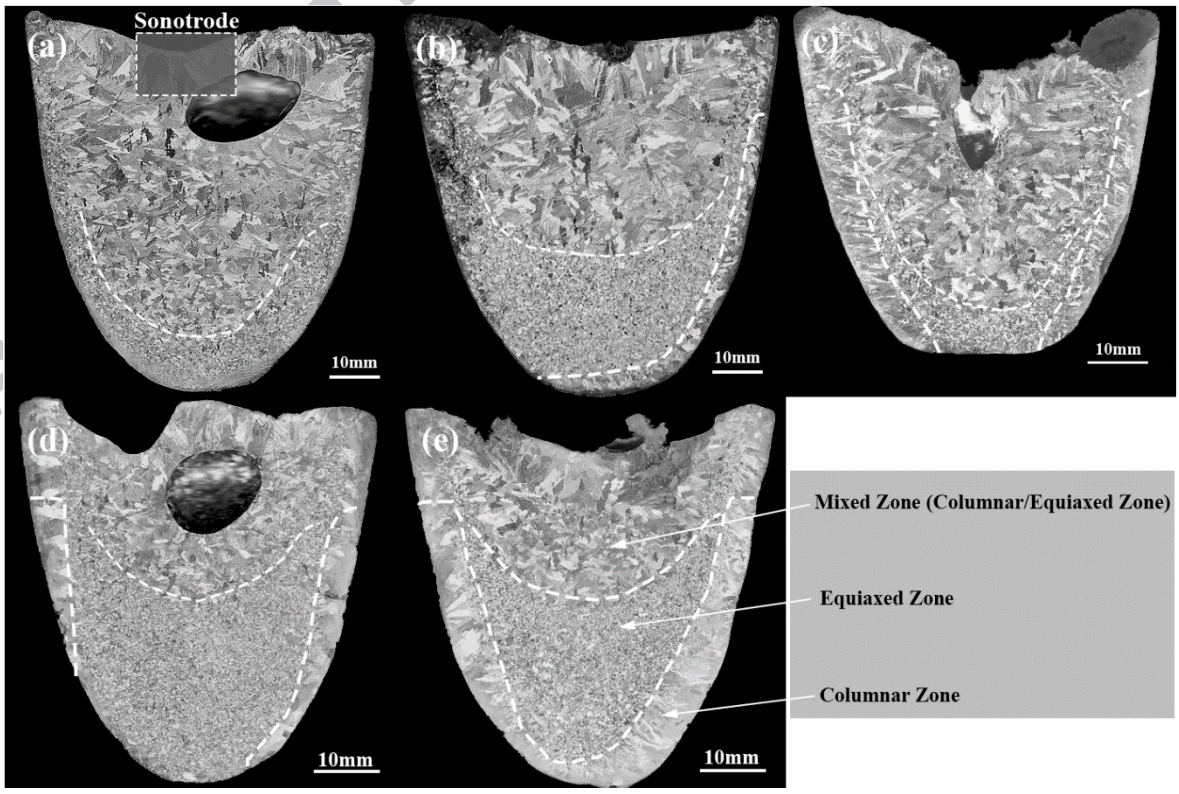

Fig. 2 Macrostructures of ultrasonically treated samples (a) T430-1M, (b) T440-2M, (c) T450-4M, (d) T440-3M and (e) T440-4M. The columnar, equiaxed and mixed (columnar/equiaxed) zones are indicated by dashed lines.

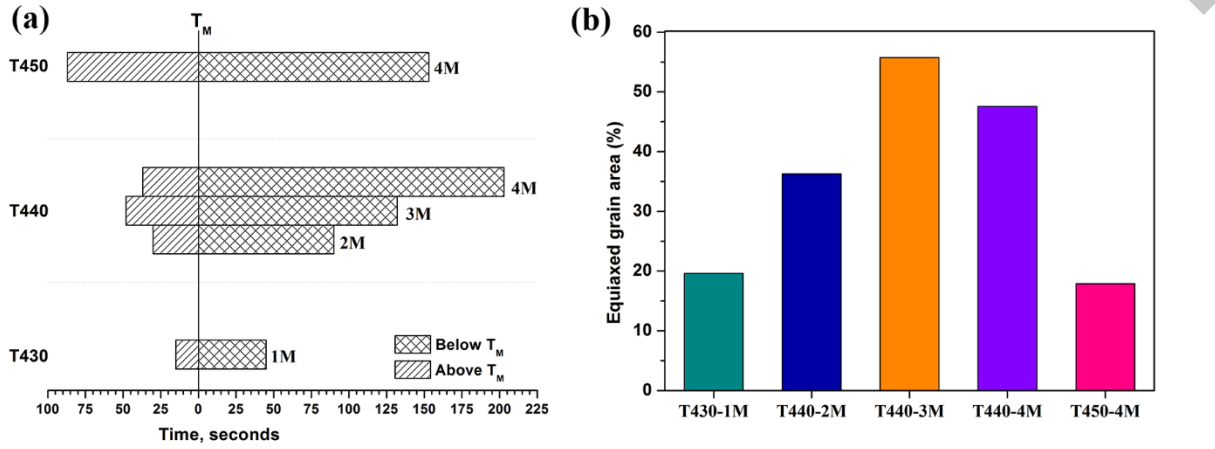

Fig. 3 (a) Time duration of UST before and after T_M and (b) the area percentage of the equiaxed zone after UST.

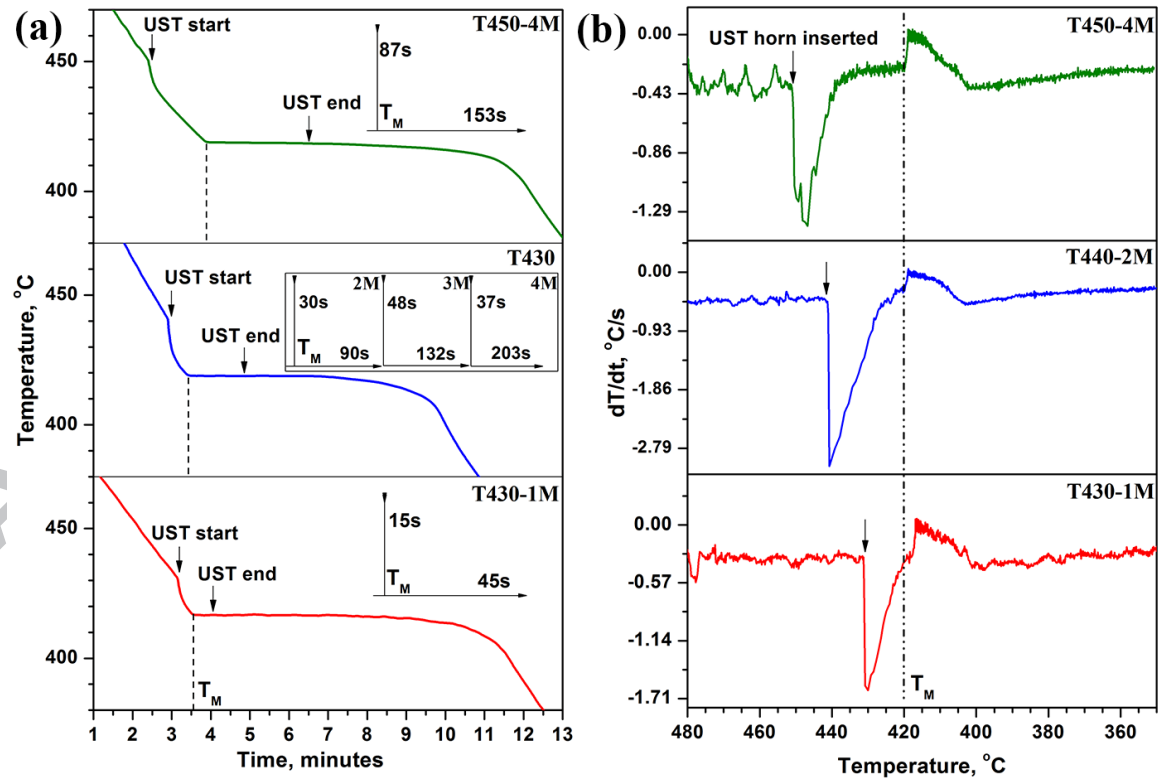

Fig. 4 (a) Cooling curves and (c) First derivative curves of samples T430-1M, T440-2M and T450-4M.

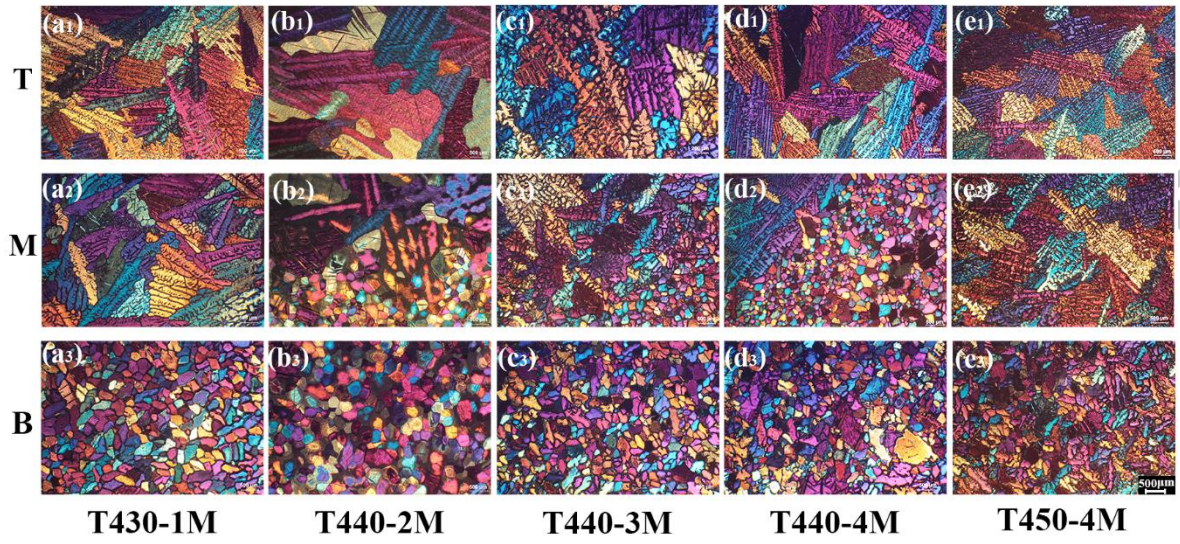

Fig. 5 Microstructures from T, M and B regions of the ultrasonically treated samples (a_1 – a_3) T430-1M, (b_1 – b_3) T440-2M, (c_1 – c_3) T440-3M, (d_1 – d_3) T440-4M and (e_1 – e_3) T450-4M.

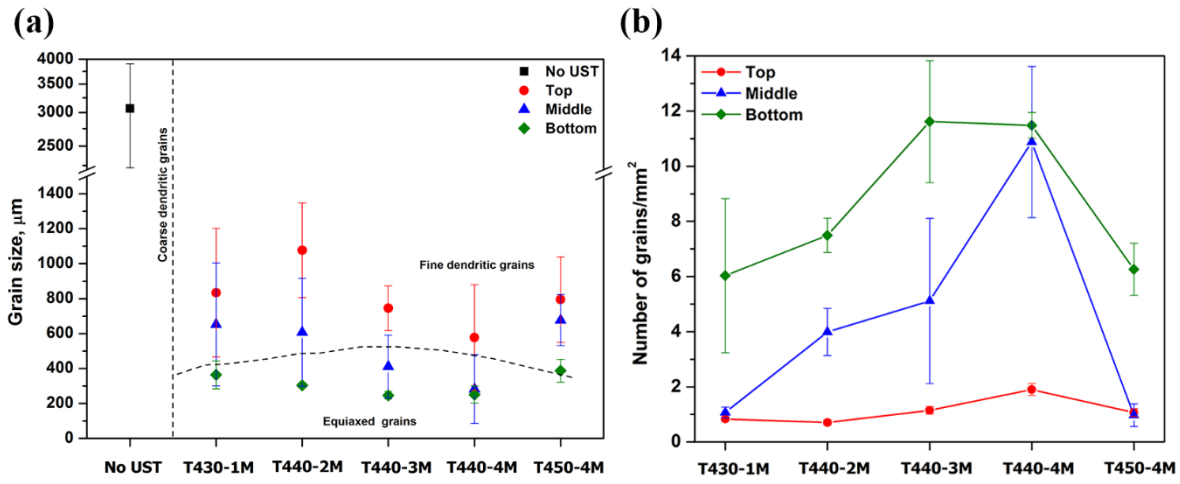

Fig. 6 (a) Average grain size measurements and (b) the number of grains per unit area measured across the samples after UST.

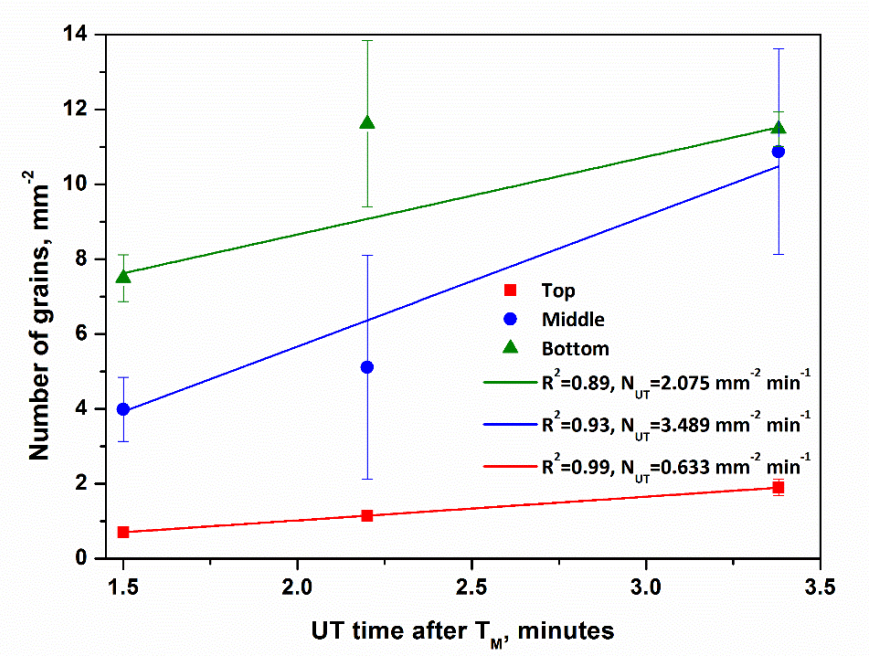

Fig. 7 The number of grains formed in regions T, M and B of samples T440-2M, 3M and 4M as a function of UST time after T_M.

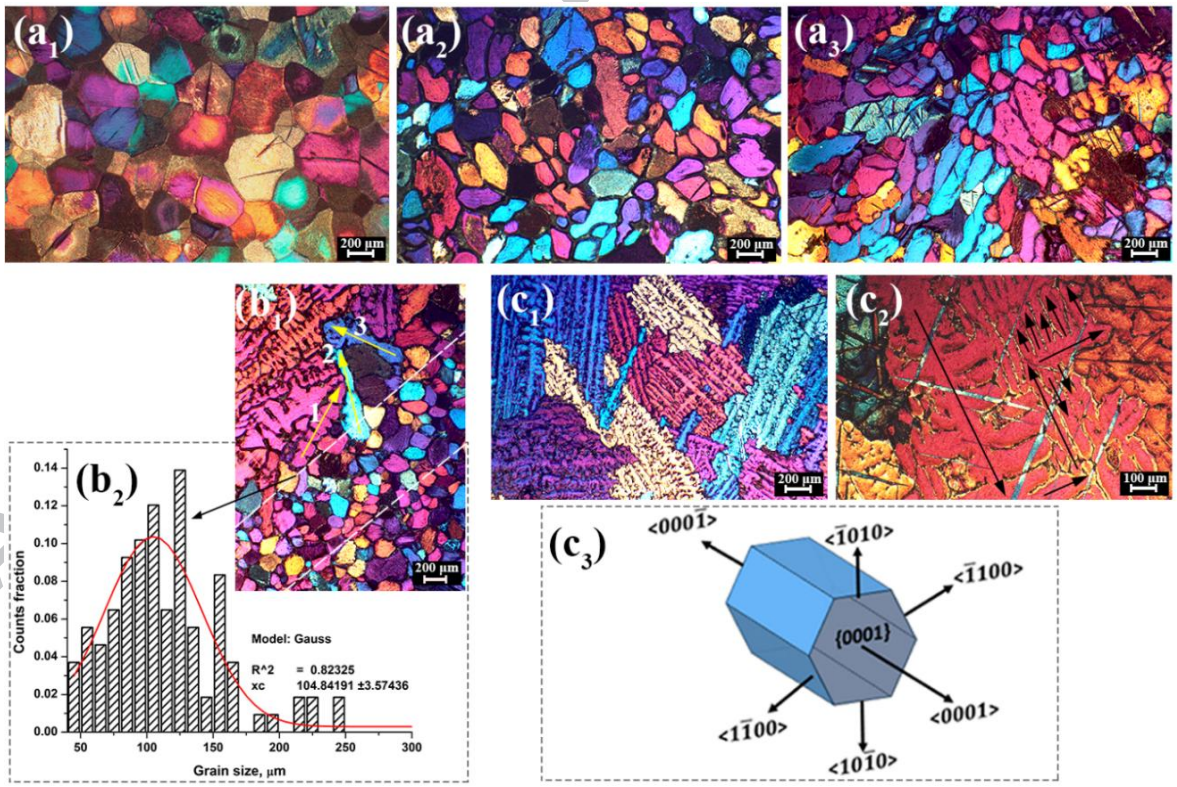

Fig. 8 (a_1 to a_3) shows the morphology of equiaxed structures in samples T440-2M, 3M and 4M respectively, (b_1 – b_2) denotes the equiaxed to dendritic transition region with size distribution and (c_1

– c_3) shows the evolution of dendritic structure and their preferential planes of growth in sample T440-4M.

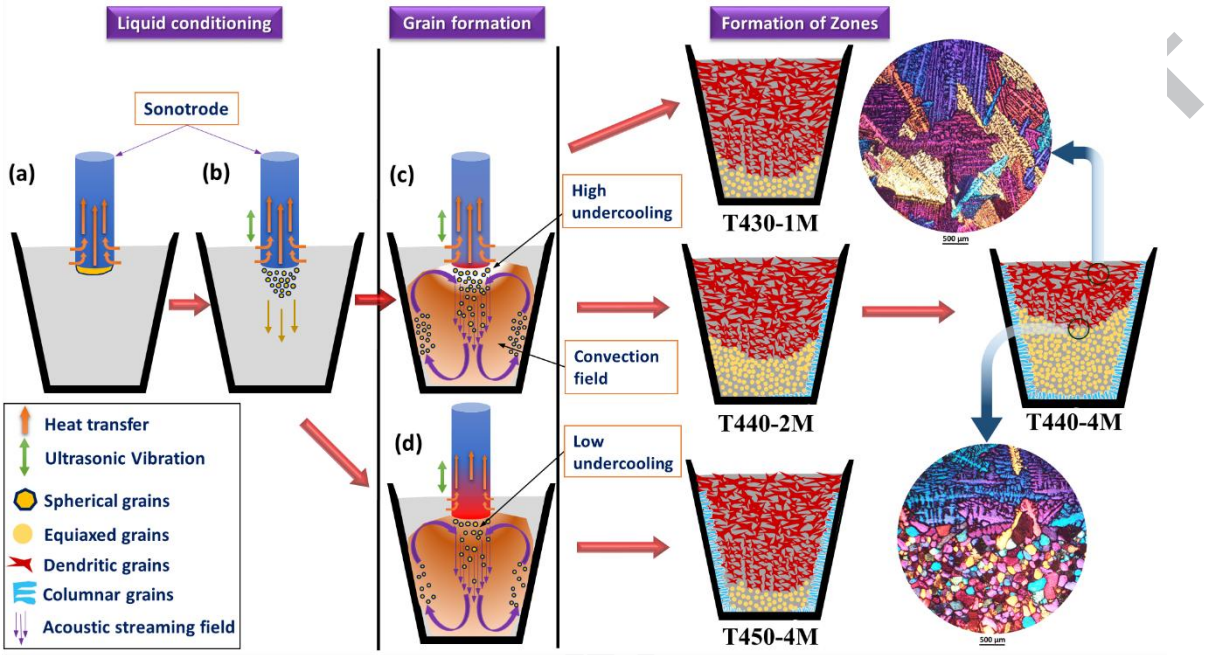

Fig. 9 Schematic illustration showing the effect of UST on the development of grain structure over a range of temperatures and times.

Table 1 Time and temperature range of the application of UST and the resultant thickness of the columnar zone and the area fraction of the equiaxed zone.

Sample code	Cast conditions	Temperature (°C)			ΔT_{UTi}	UST time (seconds)			Columnar zone thickness (mm)	Equiaxed zone (%)
		T_M	T_{UTs}	T_{UTe}	(°C)	Total T_T	Before T_M	After T_M		
-	No UST	420	–	–	–	0	0	0	0	0
T430-1M	UST	420	430	419	10	60	15	45	0	19.62
T440-2M	″	420	440	419	20	120	30	90	2.57 ± 0.51	36.27
T440-3M	″	420	440	419	20	180	48	132	2.60 ± 0.99	55.72
T440-4M	″	420	440	419	20	240	37	203	4.76 ± 0.95	47.55
T450-4M	″	420	450	419	30	240	87	153	5.03 ± 0.88	17.87

T_M – Equilibrium melting temperature of Zn

T_{UTs} – Starting temperature of UST

T_{UTe} – Ending temperature of UST

ΔT_{UTi} – Degree of superheat at UST initiation ($T_{UTs} - T_M$)

Sample code T430 to 450 represent T_{UTs} and 1M to 4M denotes the time of UST in minutes

Highlights

- Ultrasonic treatment (UST) of high purity Zn produced a grain refined structure
- Macrostructures have columnar, refined equiaxed and mixed equiaxed-columnar zones
- The number of grains produced by UST is affected by both time and temperature
- The largest equiaxed zone forms when UST is applied from 440°C for 3 or 4 minutes
- High superheat or longer UST time at low superheat reduced the number of grains

Graphical Abstract

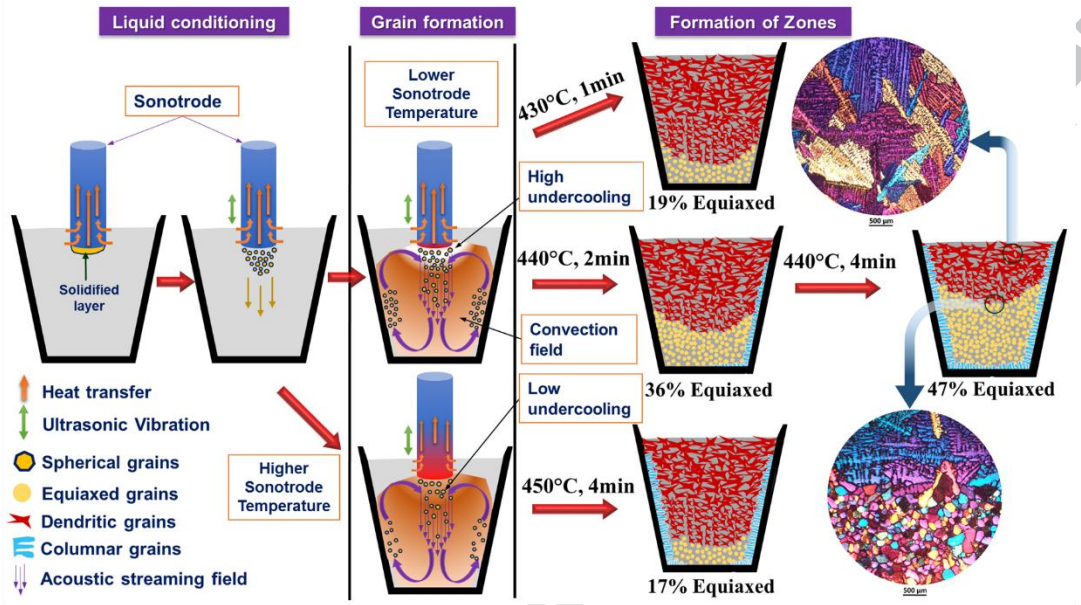

Enhanced grain formation during UST as a function of operating temperature and time in Zn solidification